Published in Applied Physics Letters 98, issue 013103, 1-4, 2005
which should be used for any reference to this work

Characterization of buried photonic crystal waveguides and microcavities fabricated by deep ultraviolet lithography

Iwan Märki,[a] Martin Salt, and Hans Peter Herzig
Institute of Microtechnology, University of Neuchâtel, rue A.-L. Breguet 2, CH-2000 Neuchâtel, Switzerland

Ross Stanley
Centre Suisse d'Electronique et de Microtechnique (CSEM), SA, Rue Jaquet-Droz 1, CH-2007 Neuchâtel, Switzerland

L. El Melhaoui, P. Lyan, and J. M. Fedeli
Laboratoire d'Electronique de Technologie de l'Information, Commissariat à l'Energie Atomique (CEA)–Grenoble, 17 rue des Martyrs, 38 054 Grenoble Cedex 9, France

We present results of the optical characterization of silicon photonic crystal waveguides and microcavities that are completely buried in a silicon dioxide cladding and are fabricated by deep ultraviolet (UV) lithography. The advantages of buried waveguides and deep UV lithography are discussed. Transmission spectra and loss factors for photonic crystal waveguides, as well as quality factors for resonant microcavities, are obtained. The observed characteristics are in good agreement with three-dimensional simulations.

I. INTRODUCTION

Photonic crystal structures are becoming important building blocks for providing exciting ways to control light and to permit further miniaturization of optical devices. Planar photonic crystals find their application, for example, in extremely small lasers, filters, multiplexers, optical switches, and microcavities.[1–4] For research purposes *e*-beam lithography is the most used technique for the fabrication of such integrated optical circuits, because of its high-resolution capabilities. However, it is expensive (per sample) and, due to its serial writing process, it is slow and therefore not suitable for mass production. Optical lithography provides the fabrication process for large volume but is limited in resolution by optical diffraction. With deep ultraviolet (UV) lithography both the resolution required to fabricate the photonic crystal structures and the parallel writing process needed for mass production have become available.[5]

In this work we present an investigation of a silicon slab photonic crystal waveguide (PCW) structure, which is completely buried in a silicon dioxide cladding. Photonic crystal structures made from silicon-on-insulator (SOI) wafers are more promising for large-scale integration because advanced complementary metal-oxide semiconductor (CMOS) fabrication technology, i.e., deep UV lithography, can be used. Photonic crystal waveguides are basic elements for building integrated optical circuits. They carry the light to and from the functional part of the photonic crystal structure (e.g., filter or resonator). The lower the losses in the PCW, the better the performance of the photonic crystal structure with the specific functionality. So far, low-loss guiding has been demonstrated in suspended membrane and low-index bottom cladding structures.[3,6] Our waveguide structures, fully buried in a silicon dioxide cladding, are protected from the environment and therefore much more practical for many applications. However, the lower refractive index contrast between the slab and the cladding makes it more difficult to achieve low-loss guiding and is a challenge during the design process. In fact, three-dimensional simulations are essential in order to precisely model the losses.

We investigate a design of a resonant microcavity inside the photonic crystal waveguide. Resonant microcavities in photonic crystals are of great interest because they exhibit highly localized optical fields and narrow transmission bands and therefore can serve as basic elements for switches, filters, and small lasers. Much effort has been spent by different groups in design and fabrication in order to improve the quality (Q) factor of microcavities. Q factors of up to 7300 have been reported for two-dimensional (2D) crystal cavities with direct in-plane transmission measurements.[3]

We report the design, fabrication, and measurement of the structures. Based on the measurements we discuss the losses in the photonic crystal waveguide and the quality factor of the resonant cavity.

II. DESIGN AND FABRICATION

First, we propose a straight photonic crystal waveguide with a W1 defect line (one row of missing holes) as a basic building block. The photonic crystal consists of a triangular array of cylindrical holes in a thin Si slab. The Si slab is completely buried in silicon dioxide.

Second, we propose a design of in-plane resonant cavity, which is formed by two identical Bragg reflectors and is situated inside the photonic crystal waveguide (see Fig. 1). The design parameters of the Bragg reflectors are different from those of the rest of the photonic crystal, thus increasing

[a]Electronic mail: iwan.maerkl@unine.ch

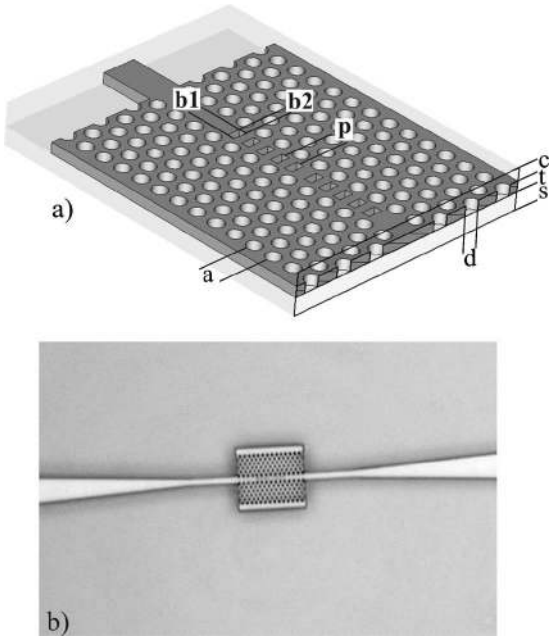

FIG. 1. (a) In-plane photonic crystal microcavity structure buried in silicon dioxide (PC period $a=490$ nm, hole diameter $d=350$ nm, core thickness $t=238$ nm, bottom oxide thickness $s\approx2000$ nm, and upper cladding thickness $c\approx700$ nm). The microcavity inside the photonic crystal waveguide is formed by two five-hole Bragg reflectors (hole dimensions $b1=325$ nm and $b2=180$ nm, period $p=373$ nm). (b) Optical microscope image of the fabricated waveguide structure showing the tapered sections guiding the light to and from the photonic crystal microcavity.

the design options for the cavity. The cavity structure is designed so as to obtain a highly localized field inside the cavity and high in-plane transmission for a narrow frequency band. In order to achieve a high-Q factor and high in-plane transmission, the radiation losses, i.e., the modal mismatch at the interface between the photonic crystal waveguide and the cavity structure, need to be minimized by engineering the hole dimensions and positions of the Bragg reflectors during the design process. Several methods have been suggested for optimizing the performance of photonic crystal microcavities, including tapering,[7] Bloch-wave engineering[8] or radiation losses recycling.[9] All these methods require very high accuracy and quality in the fabrication. Being at the limit of the possible resolution with deep UV lithography, we have kept the design as simple as possible while accepting lower performance for the photonic crystal cavity. The holes forming the Bragg reflectors are all equally spaced and have the same dimensions. A microcavity with four holes on both sides and a microcavity with five holes on both sides have been fabricated and measured.

The photonic crystal structures are fabricated by Laboratoire d'Electronique de Technologie de l'Information (LETI), France using deep UV lithography at a wavelength of 193 nm. After the lithographic process, the patterns in the photoresist are transferred into the silicon layer of the SOI wafer using dry etching technology. As a final step, the etched structures in the silicon are then covered with an oxide layer.

III. MEASUREMENTS

Measurements are performed with an optical setup that includes a tunable laser source. An aspheric lens is used to inject TE-polarized light (in-plane polarization) into a 10 -μm-wide, 238-nm-thick silicon layer buried in silicon dioxide. The light is guided via a taper, which reduces the waveguide width to 0.5 μm, to the photonic crystal waveguide. In the case of the W1 waveguide the light is directly transmitted, whereas in the case of the microcavity the light couples into the resonant cavity for a narrow frequency band, where it is highly localized and eventually transmitted. Using a second, identical taper the transmitted light is then guided to the exit of the device, where it is collected by a microscope objective and focused onto an InGaAs detector for measurements. The tunable laser source allows us to measure the transmission spectrum ranging from 1440 to 1590 nm.

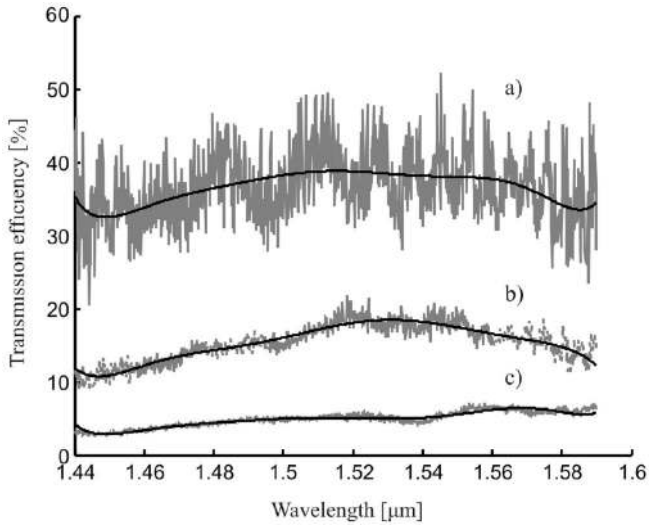

FIG. 2. Filtered (black) and nonfiltered (gray) normalized transmission spectra of three W1 waveguide samples of different lengths: (a) 41a, (b) 81a, and (c) 161a, with $a=490$ nm. The oscillations in the nonfiltered transmission spectra are due to the reflections at the end facets forming the periodic Fabry–Pérot interference pattern.

The measured transmission spectra contain a dominant periodic Fabry–Pérot interference pattern (see Fig. 2), which corresponds to the total length of the waveguide system and is due to the reflections at the smooth waveguide end facets. To obtain the approximate transmission efficiency of the photonic crystal waveguide and the resonant microcavity, we first remove numerically the Fabry–Pérot interference pattern from the measurement data by filtering the peak corresponding to the total waveguide length in the Fourier-transformed spectrum. Second, we divide the transmission spectra by the spectrum of a straight reference waveguide for normalization. The reference waveguide has a width of 10 μm and a thickness of 238 nm, which corresponds exactly to the PC waveguide without tapered and photonic crystal sections. This eliminates extrinsic effects of the end injection and most of the spectral response of the measurement optics.

In Fig. 2 we show the filtered and nonfiltered normalized transmission spectra of three W1 waveguide samples of different lengths (41a, 81a, and 161a, with $a=490$ nm). They exhibit an even transmission spectrum over the whole measurement range from 1440 to 1590 nm with a variation of $\pm10\%$. In the case of the shortest PCW (41a) about 35% of the light that is coupled from free space into the input end

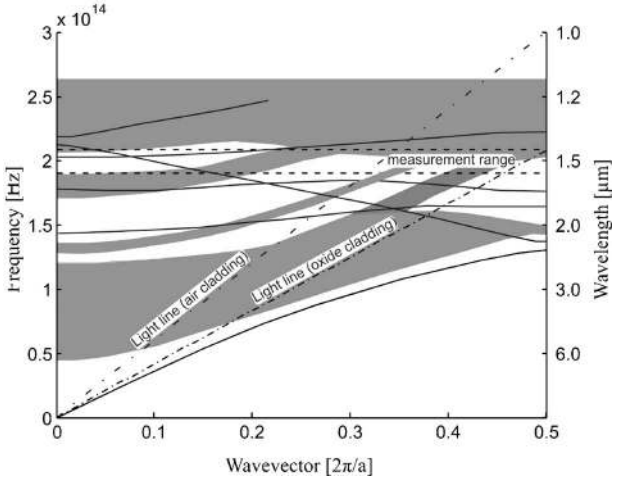

FIG. 3. Dispersion diagram for TE-like guided modes in the W1 PC waveguide obtained by a fully three-dimensional calculation based on a plane-wave expansion method. The defect modes are represented by the solid black lines. The dark gray regions correspond to modes of the photonic crystal, which are states that can propagate through the crystal. The modes above the light line will leak energy into the cladding (leaky modes).

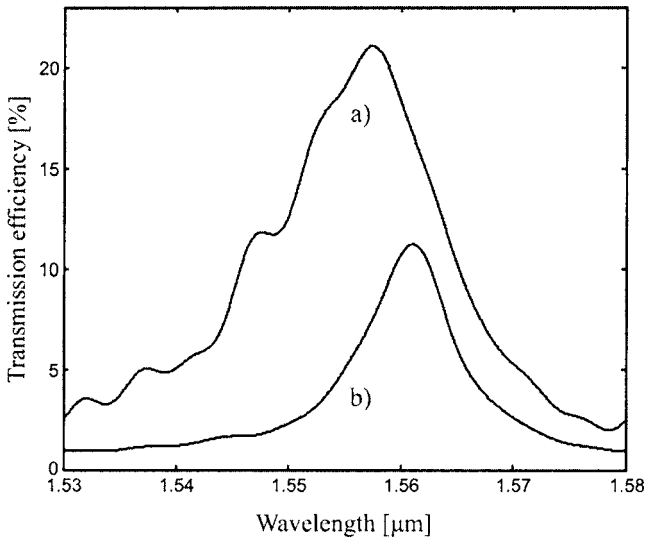

FIG. 4. Measured transmission spectrum of (a) a four-hole reflector cavity and (b) a five-hole reflector cavity. The raw measurement data have been filtered to remove the Fabry–Pérot interference.

face of the 10-μm-wide waveguide is transmitted. As mentioned above, the lower refractive index contrast between the slab and the cladding makes it more difficult to achieve low-loss guiding. The computed dispersion diagram, shown in Fig. 3, illustrates the more limited possibilities for low-loss guiding below the light line due to the oxide cladding. For comparison, the light line for an air cladding is indicated as well. The different guided defect modes, shown in Fig. 3, are represented by the solid black lines. We observe that the present design does not posses a suitable propagating mode in the measurement range that is below the light line. Therefore, the longer the PCW the more light is leaking vertically. In fact, the contrast in the Fabry–Pérot interference pattern of the nonfiltered transmission spectra is proportional to the averaged transmission efficiency (filtered value), indicating the loss induced by the PCW. In order to calculate the propagation losses we compare the different transmission efficiencies depending on the different lengths of the photonic crystal waveguides using the cutback method.[10] We obtained a propagation loss of 150 dB/mm. The transmission measurements have been repeated several times in order to confirm the obtained propagation loss value. Accordingly, the error is estimated to ±30 dB/mm. In comparison, we have performed three-dimensional simulations using a finite integration time domain (FITD) algorithm.[11] They have shown a propagation loss of 100 dB/mm, indicating that there are some extra losses in the real system, coming from, e.g., surface roughness. By adequately changing the design of the PCW, such as the silicon slab thickness and the PC waveguide width, it is possible to shift the propagating mode into the limited region below the light line (see Fig. 3), which would allow nonradiative vertical guiding, i.e., a significant reduction in vertical loss. Improvements in fabrication such as higher accuracy in dimensions and smoother sidewalls will result in a reduction of the scattering losses. In addition, based on the propagation loss we estimate the losses at the interface between the conventional waveguide and the photonic crystal waveguide to be about 35%. These losses can be reduced by varying the width of the conventional waveguide[12] or by introducing a taper system[13] for a better mode matching.

In Fig. 4 we show the measured spectral response of two different in-plane resonant cavities inside the W1 PCW: One cavity with Bragg reflectors formed by four holes on both sides of the cavity and one cavity with Bragg reflectors formed by five holes on both sides of the cavity (Fig. 1). For the four-hole cavity we observe a transmission peak at $\lambda \sim 1557$ nm and an approximate maximum transmission efficiency at resonance of 21%. The measured quality factor $Q \sim \lambda/\Delta\lambda_{\mathrm{FWHM}}$ is equal to 100. The weak modulation on the left part of the spectrum is likely due to fabrication-induced nonuniformities in the cavity structure. Such modulations have also been observed in our three-dimensional simulations when varying the hole dimensions and positions of the Bragg reflectors inside the PCW. The transmission spectrum of the five-hole cavity is much narrower and more Lorentzian-like than the spectrum of the four-hole cavity. We observe an approximate maximum transmission efficiency of about 11% at a slightly higher peak wavelength (1562 nm) induced by a small increase in the effective cavity length due to the presence of the additional Bragg holes. The measured quality factor $Q \sim \lambda/\Delta\lambda_{\mathrm{FWHM}}$ is equal to 200. Thus, by adding one hole to the Bragg reflectors on both sides of the microcavity we can increase the quality by a factor of 2, whereas the transmission efficiency is reduced by approximately that same factor. In Fig. 5 we show the corresponding three-dimensional (3D) simulated transmission efficiencies of the two different microcavities using the 3D FITD algorithm.[11] The quality factor for the four-hole cavity is 240 and for the five-hole cavity is 440. The maximum transmission efficiencies are 41% and 17%, respectively. Compared to the measurements, the simulated values are about two times better. Additionally, we note the asymmetry and the higher resonant wavelengths in the measured transmission spectra. The observed differences between Figs. 4 and 5 are

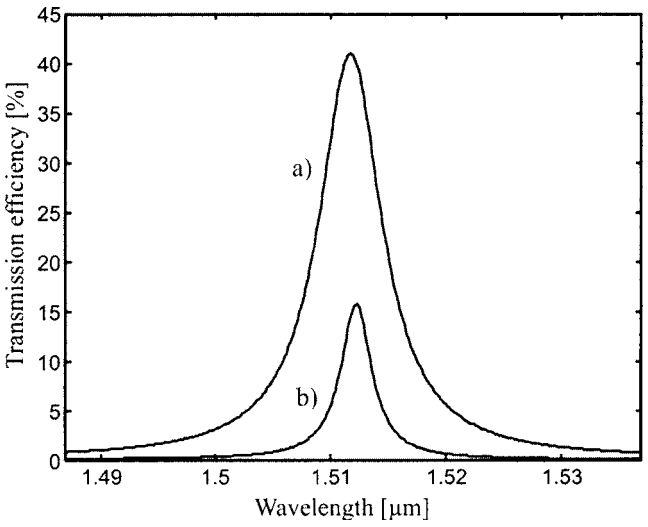

FIG. 5. Simulated transmission efficiency of (a) a four-hole reflector cavity and (b) a five-hole reflector cavity.

due to variations between the fabricated structure and the ideal simulated structure. Small defects, such as variations in the hole dimensions or sidewall roughness, also induce higher losses, which cause a reduction in transmission and in the quality factor. However, despite the difference in the absolute values, the ratio between the two quality factors and the two maximum transmission efficiencies observed in the measured spectrum is in very good agreement with that of the simulated spectra. Our simulations have shown that by adding one hole to the reflectors on both sides of the microcavity, the reflectivity increases by 10%. Therefore, on the one hand the quality factor increases and on the other hand the transmission efficiency decreases because more light is either reflected back to the input end face or scattered into the cladding.

Based on the loss calculation of the W1 waveguides, we can evaluate the losses induced by the microcavity. The losses attributed to the four-hole cavity and the five-hole cavity are in the order of 25% and 38%, respectively. These losses include scattered light and light that is reflected back to the input end facet. With a modified design for the PC waveguide providing a propagating mode below the oxide cladding light line, the losses induced by the microcavity can as well be reduced. The quality factor of the microcavity can be improved by further increasing the reflectivity of these mirrors. However, the reflectors must be designed such as to allow efficient coupling between the photonic crystal waveguide mode and the resonant cavity mode. As mentioned earlier, this can be achieved by using different design methods.

IV. CONCLUSION

We have investigated a W1 photonic crystal waveguide and a design of an in-plane resonant cavity completely buried in silicon oxide and fabricated by deep UV lithography. On the one hand, the buried photonic crystal structure is well protected and therefore very promising for applications. On the other hand, the oxide cladding makes it more difficult to achieve low-loss guiding. By changing the silicon slab thickness and the PC waveguide width it should be possible to achieve low-loss guiding with a propagating mode below the light line. We have presented transmission measurements for PCW and cavities in silicon dioxide. For the W1 waveguide, a loss of 150 dB/mm has been measured. The quality factor for the resonant microcavities was measured to be about 100 for the four-hole cavity and about 200 for the five-hole cavity. The transmission measurements for the microcavities are in good agreement with the 3D FITD simulations. Further improvements to the maximum transmission efficiency and the quality factor of the resonant cavities can be achieved by optimizing the design of the photonic crystal waveguide and of the reflectors forming the microcavity.

Besides design optimization, our future investigations will focus on the strong localization of the optical field in a microcavity, which is sensitive to small perturbations and can lead to significant changes in the transmission properties.

[1] A. Mekis, J. C. Chen, I. Kurland, S. Fan, P. Villeneuve, and J. D. Joannopoulos, Phys. Rev. Lett. **77**, 3787 (1996).
[2] S. Fan, P. Villeneuve, and J. D. Joannopoulos, Opt. Express **3**, 4 (1998).
[3] M. Notomi, A. Shinya, S. Mitsugi, E. Kuarmochi, and H.-Y. Ryu, Opt. Express **12**, 1551 (2004).
[4] M. Lončar, T. Yoshie, and A. Scherer, Appl. Phys. Lett. **81**, 2680 (2002).
[5] W. Bogaerts *et al.*, Opt. Express **12**, 1583 (2004).
[6] S. J. McNab, N. Moll, and Y. A. Vlasov, Opt. Express **11**, 2927 (2003).
[7] M. Palamaru and Ph. Lalanne, Appl. Phys. Lett. **78**, 1466 (2001).
[8] Ph. Lalanne and J. P. Hugonin, IEEE J. Quantum Electron. **39**, 1430 (2003).
[9] Ph. Lalanne, S. Mias, and J. P. Hugonin, Opt. Express **12**, 458 (2004).
[10] M. Notomi, A. Shinya, K. Yamada, J. Takahashi, C. Takahashi, and I. Yolohama, IEEE J. Quantum Electron. **38**, 736 (2002).
[11] T. Weiland, Int. J. Numer. Model. **9**, 295 (1996).
[12] W. Kuang and J. D. O'Brien, Opt. Lett. **29**, 860 (2004).
[13] A. Talneau, M. Mulot, S. Anand, and Ph. Lalanne, Appl. Phys. Lett. **82**, 2577 (2003).